Powder diffraction intensities of α-Al_2O_3 calculated by traditional & DFT calculations

Takashi Ida
Advanced Ceramics Research Center, Nagoya Institute of Technology, Japan
ida.takashi@nitech.ac.jp

Introduction

ICDD PDF-4+ 2023 lists 23 star-quality data sets of corundum (α-Al_2O_3), where 21 sets (00-046-1212, 01-070-5679, 01-070-7364, 01-071-1683, 01-075-1862, 01-075-1863, 01-075-6775, 01-082-1399, 01-088-0286, 01-089-7715, 04-004-2852, 04-004-5434, 04-005-4213, 04-005-4505, 04-007-1400, 04-007-4873, 04-015-8608, 04-015-8993, 04-015-8994, 04-015-8995 & 04-015-8996) assign the strongest peak to 104-reflection,
and 2 sets (01-089-7716 & 01-089-7717) assign the strongest peak to 113-reflection.

NIST certifies 113-reflection is the strongest, 116-reflection is the 2nd strongest, and 104-reflection is the 3rd strongest for SRM676a standard α-Al_2O_3 powder, while 104-reflection is the strongest, 116-reflection is the 2nd strongest, and 1.0.10/119-reflections are the 3rd strongest for standard α-Al_2O_3 sintered disk SRM1976c.

Hubbard et al. (1976) have shown that it is expected that 116-reflection should be the strongest, 113-reflection the 2nd strongest, and 104-reflection the 3rd strongest for a neutral atom model $Al_2^0O_3^0$, while 113-reflection should be the strongest, 116-reflection the 2nd strongest, and 104-reflection the 3rd strongest for a fully-ionized model $Al_2^{3+}O_3^{2-}$.

Crystallographic Data of Corundum

Trigonal, $R\bar{3}c$ (No. 167), $a = 4.759$ Å, $c = 12.993$ Å (hexagonal setting)

$c/a = 2.73$ (α-Al_2O_3) $\gg \sqrt{6} \approx 2.45$ (ideal hcp arrangement of oxygen)

$B_{iso} \equiv 8\pi^2 U_{iso} \approx 0.22$ Å^2 $\Leftrightarrow$ $U_{iso} = 0.0028$ Å^2

TABLE I. Atomic positions and mean square displacements of α-Al_2O_3 from 5 data sets for 2 single crystals (Maslen et al., 1993)

	Crystal 1		Crystal 2		
	Data (1)	Data (2)	Data (3)	Data (4)	Data (5)
z (Al)	0.352 2	0.352 2	0.352 2	0.352 2	0.352 2
x (O)	0.694 2	0.693 8	0.693 8	0.694 0	0.694 0
U_{11} (Al) (Å^2)	0.002 4	0.002 1	0.002 5	0.002 5	0.002 5
U_{33} (Al) (Å^2)	0.002 7	0.002 5	0.002 4	0.002 4	0.002 4
U_{11} (O) (Å^2)	0.002 8	0.002 5	0.002 8	0.002 8	0.002 8
U_{22} (O) (Å^2)	0.002 7	0.002 6	0.003 0	0.003 0	0.003 0
U_{33} (O) (Å^2)	0.002 7	0.002 8	0.002 8	0.002 8	0.002 8
U_{12} (O) (Å^2)	0.000 3	0.000 3	0.000 3	0.000 3	0.000 3

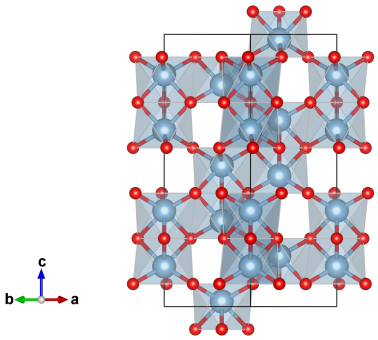

Figure 1. Projection of α-Al_2O_3 structure along [110]-direction in hexagonal setting, drawn with *VESTA 3* (Momma & Izumi, 2011)

Density Functional Theory (DFT) Calculation

Quantum ESPRESSO 7.1 (Gianozzi et al., 2009, 2017) (open-source, free)

Pseudo-potential: projector-augmented wave (PAW) (Kresse & Joubert, 1999)

Exchange-correlation: local density approximation (LDA) (Perdew & Zunger, 1981) & Perdew-Burke-Ernzerhof (PBE) model (Perdew et al., 1996, 1997)

Electron density: 60 × 60 × 60-mesh for rhombohedral (reduced) cell ($a = 5.129$ Å, $\alpha = 55.29°$)

↓ (Fourier transform + Dispersion correction) × (Common atomic displacement)

↓ (Square absolute, Geometrical correction, Sum of equivalent reflections)

XRD peak intensities, I_{hkl}

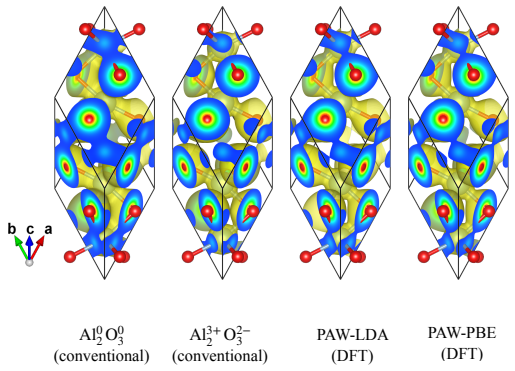

Figure 2. Projection of electron density iso-surface (yellowish color) at the level of 0.3 e/Å^3 along [11$\bar{2}$]-direction in rhombohedral setting, and color-scaled density map (red: high, blue: low) on the faces of the rhombohedral cell, rendered from 60 × 60 × 60 voxel data with *VESTA 3* (Momma & Izumi, 2011)

Experimental & Treatment of XRD Data

Powder #1 (High Purity Chemicals, 99.99%, 2–3 μm)
Powder #2 (High Purity Chemicals, 99.99+%, ca 0.3 μm)

Instrument: Rigaku MiniFlex (Cu $K\alpha$) with silicon-strip X-ray detector

Deconvolutional Treatment (DCT) (Ida, 2021a)

Individual peak profile fitting with a symmetric profile function (Ida, 2021b)

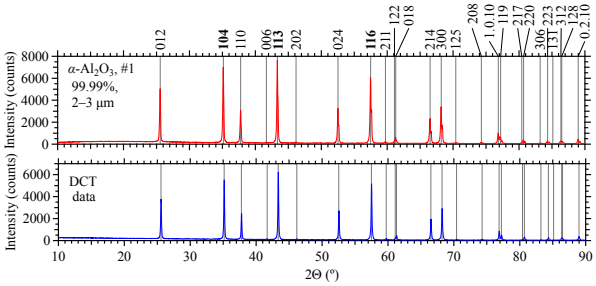

Figure 3. Observed (upper; red) and deconvolutionally treated (DCT) (lower; blue) X-ray diffraction intensity of α-Al_2O_3. Vertical lines indicate the peak locations listed in PDF 00-046-1212.

Figure 4. Demonstration of DCT and automatic individual peak profile fitting with a symmetric function for 113-reflection of α-Al_2O_3; w: HWHM of Lorentzian component, σ & k: standard deviation & excess kurtosis of symmetrized instrumental function.

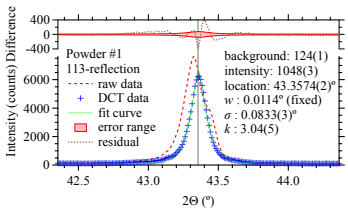

TABLE II. XRD relative intensities listed in ICDD PDF-4+, intensities certified for NIST SRM676a & SRM1976c, intensities for $Al_2^0O_3^0$, $Al_2^{1.5+}O_3^-$ & $Al_2^{3+}O_3^{2-}$ calculated by a conventional method, intensities calculated by DFT (PAW-LDA & PAW-PBE) methods, and intensities extracted from experimental data. Values in parentheses are differences from NIST SRM676a data. Strongest 2nd Strongest 3rd Strongest

hkl	ICDD PDF-4+		NIST		Conventional			DFT		Experimental	
	00-046-1212	01-089-7716	SRM 676a	SRM 1976c	$Al_2^0O_3^0$	$Al_2^{1.5+}O_3^-$	$Al_2^{3+}O_3^{2-}$	PAW LDA	PAW PBE	99.99% 2–3 μm	99.99+% ca 0.3 μm
012	45 (–12)	65.7 (+8.6)	57.1	24 (–33)	61.0 (+3.9)	59.3 (+2.2)	57.1 (+0.0)	54.1 (–3.0)	57.3 (+0.2)	56.8 (–0.3)	56.7 (–0.4)
104	100 (+12)	99.5 (+11.1)	88.4	100 (+12)	97.5 (+9.1)	94.5 (+6.1)	90.8 (+2.4)	79.8 (–8.6)	84.3 (–4.1)	87.3 (–1.1)	90.0 (+1.6)
110	21 (–17)	46.4 (+8.6)	37.8		45.6 (+7.8)	43.3 (+5.5)	40.8 (+3.0)	32.5 (–5.3)	34.0 (–3.8)	37.2 (–0.6)	36.0 (–1.8)
113	66 (–34)	100	100	37 (–63)	98.0 (–2.0)	99.4 (–0.6)	100	100	100	100	100
024	34 (–13)	48.0 (+0.7)	47.3	21 (–26)	50.5 (+3.2)	50.8 (+3.5)	50.7 (+3.4)	43.0 (–4.3)	42.7 (–4.6)	46.3 (–1.0)	45.7 (–1.6)
116	89 (–7)	94.2 (–1.6)	95.8	88 (–8)	100 (+4.2)	100 (+4.2)	99.3 (+3.5)	86.7 (–9.1)	88.2 (–7.6)	92.6 (–3.2)	95.2 (–0.6)
214	23 (–15)	35.1 (–2.6)	37.7		40.5 (+2.8)	40.6 (+2.9)	40.5 (+2.8)	33.3 (–4.4)	33.1 (–4.6)	36.1 (–1.6)	34.9 (–2.8)
300	27 (–31)	54.1 (–3.4)	57.5	12 (–46)	61.9 (+4.4)	61.5 (+4.0)	60.6 (+3.1)	53.0 (–4.5)	52.7 (–4.8)	56.4 (–1.1)	52.3 (–5.2)
δ_{RMS}	20%	6.0%		37%	5.2%	3.9%	2.6%	5.6%	4.4%	1.4%	2.3%

δ_{RMS} : Root mean square difference from NIST SRM676a intensities